arXiv:1410.3049v1 [quant-ph] 12 Oct 2014

Circuit QED: Implementation of the three-qubit refined Deutsch-Jozsa quantum algorithm

Qi-Ping Su and Chui-Ping Yang

Department of Physics, Hangzhou Normal University,

Hangzhou, Zhejiang 310036, China

(Dated: October 14, 2014)

Abstract

We propose a protocol to construct the 35 f-controlled phase gates of a three-qubit refined Deutsch-Jozsa (DJ) algorithm, by using single-qubit σ_z gates, two-qubit controlled phase gates, and two-target-qubit controlled phase gates. Using this protocol, we discuss how to implement the three-qubit refined DJ algorithm with superconducting transmon qutrits resonantly coupled to a single cavity. Our numerical calculation shows that implementation of this quantum algorithm is feasible within the present circuit QED technique. The experimental realization of this algorithm would be an important step toward more complex quantum computation in circuit QED.

PACS numbers: 03.67.Lx, 42.50.Dv, 85.25.Cp

I. INTRODUCTION

As one of the most promising solid-state candidates for quantum information processing [1,2], the physical system composed of circuit cavities and superconducting qubits is of particular interest. This is because: (i) superconducting qubits and microwave resonators (a.k.a. cavities) can be fabricated using modern integrated circuit technology, and their properties can be characterized and adjusted in situ, (ii) superconducting qubits have relatively long decoherence times [3,4], and (iii) a superconducting microwave cavity or resonator plays a role of quantum bus which can mediate long-range and fast interaction between distant superconducting qubits [5-7]. Moreover, the strong coupling between the cavity field and superconducting qubits, which is difficult to implement with atoms in a microwave cavity, was earlier predicted in theory [1,8] and has been experimentally demonstrated [9,10]. Because of these features, circuit QED has been widely utilized for quantum information processing. Based on circuit QED, many theoretical proposals have been presented for realizing two-qubit gates [5,11-18] and multiple qubit gates [19-20] with superconducting qubits. Moreover, experimental demonstration of two-qubit gates [6,7,21,22] and three-qubit gates [23-25] with superconducting qubits in circuit QED has been also reported.

The interest in quantum computation is stimulated by the discovery of quantum algorithms [26,27] which can solve problems of significance much more efficiently than their classical counterparts. Among important quantum algorithms, there exist the Deutsch algorithm [28], the Deutsch-Jozsa algorithm [29], the Shor algorithm [30], the Simon algorithm [31], the quantum Fourier transform algorithm, and the Grover search algorithm [32]. As is well known, the Deutsch algorithm and the Deutsch-Jozsa algorithm were the first two that make use of the features of quantum mechanics for quantum computation. Compared with other quantum algorithms, these two algorithms are easy to be implemented and thus have been considered as the natural candidates for demonstrating power of quantum computation.

We note that with superconducting qubits coupled to a circuit cavity, a *two-qubit Deutsch-Jozsa* quantum algorithm and a two-qubit Grover search quantum algorithm were previously demonstrated in experiments [7]. However, after a thorough investigation, we note that how to implement a *three-qubit* Deutsch-Jozsa (DJ) quantum algorithm with superconducting qubits or qutrits in circuit QED has not been reported in both theoretical and experimental aspects. As is known, the experimental realization of the three-qubit DJ algorithm with a

cavity-superconducting-device system is important because it would be an important step toward more complex quantum computation in circuit QED.

In this paper, we propose a protocol to construct the 35 f-controlled phase gates of a three-qubit refined DJ algorithm, by using single-qubit σ_z gates, two-qubit CP gates, and two-target-qubit CP gates. It should be noted that a two-target-qubit CP gate consists of two sequential controlled σ_z gates, which have a common control qubit but a different target qubit. The protocol is quite general and can be applied to implement the three-qubit DJ algorithm in various of physical systems. Based on this protocol, we further discuss how to implement the three-qubit refined DJ algorithm with superconducting transmon qutrits resonantly coupled to a single cavity. Our numerical calculation shows that implementation of this quantum algorithm is feasible within the present circuit QED technique.

The paper is organized as follows. In Sec. II, we review the refined DJ algorithm. In Sec. III, we present a protocol to construct the 35 f-controlled phase gates. In Sec. IV, we discuss how to implement this DJ algorithm with superconducting transmon qutrits coupled to a cavity via resonant interaction, and analyze the experimental feasibility. A concluding summary is given in Sec. V.

II. REFINED DEUTSCH-JOZSA ALGORITHM

The DJ algorithm is aimed at distinguishing the constant function from the balanced functions on 2^n inputs. The function $f(x)$ takes either 0 or 1. For the constant function, the function values are constant (0 or 1) for all 2^n inputs. In contrast, for the balanced function, the function values are equal to 1 for half of all the possible inputs, and 0 for the other half. Using the DJ algorithm, whether the function is constant or balanced can be determined by only one query. However, a classical algorithm would require $2^{n-1}+1$ queries to answer the same problem, which grows exponentially with input size.

The refined DJ algorithm was proposed by Collins *et al.* in 2001 [33], which is illustrated in Fig. 1. This refined DJ algorithm is described below:

(i) Each input query qubit is prepared in the initial state $|0\rangle$.

(ii) Perform a Hadamard transformation H on each qubit, resulting in $|0\rangle \rightarrow (|0\rangle+|1\rangle)/\sqrt{2}$ and $|1\rangle \rightarrow (|0\rangle-|1\rangle)/\sqrt{2}$). As a result, the n-qubit initial state $|00\cdots0\rangle$ changes to the state $\frac{1}{2^{n/2}}\sum_{x=0}^{2^n-1}|x\rangle$ (denoted as $|\psi_1\rangle$).

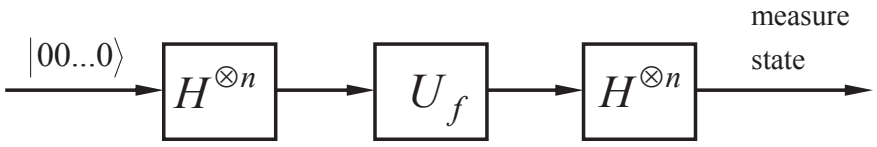

FIG. 1: Quantum circuit for the refined n-qubit Deutsch-Jozsa algorithm.

(iii) Apply the f-controlled phase shift U_f, described by

$$|x\rangle \xrightarrow{U_f} (-1)^{f(x)} |x\rangle , \tag{1}$$

which leads the state $|\psi_1\rangle$ to the state $\frac{1}{2^{n/2}} \sum_{x=0}^{2^n-1} (-1)^{f(x)} |x\rangle$ (denoted as $|\psi_2\rangle$).

(iv) Perform another Hadamard transformation H on each qubit. As a result, the state $|\psi_2\rangle$ becomes $\frac{1}{2^n} \sum_{z=0}^{2^n-1} \sum_{x=0}^{2^n-1} (-1)^{x\cdot z+f(x)} |z\rangle$.

(v) Measure the final state of the n qubits. If the n qubits are measured in the state $|00...0\rangle$, then $f(x)$ is constant. However, if they are measured in other n-qubit computational basis states, then $f(x)$ is balanced. This is because the amplitude $a_{|00...0\rangle}$ of the state $|00...0\rangle$ is given by $a_{|00...0\rangle} = \frac{1}{2^n} \sum_{x=0}^{2^n-1} (-1)^{f(x)}$, which is ± 1 for a constant $f(x)$ while 0 for a balanced $f(x)$.

One can see that when compared with the original DJ algorithm [29], this refined DJ algorithm does not need an auxiliary working qubit. Hence, it requires one qubit fewer than the original DJ algorithm. Consequently, its physical implementation requires one fewer two-state system.

III. PROTOCOL FOR CONSTRUCTION OF THE f-CONTROLLED PHASE GATES

For a n-qubit DJ algorithm, there are a total of $C_{2^n}^{2^{n-1}}$ balanced functions, among which only $C_{2^n}^{2^{n-1}}/2$ balanced functions are nontrivial if the symmetry is taken into account. For the three-qubit DJ algorithm, i.e., $n = 3$, there thus exist $C_8^4/2 = 35$ nontrivial balanced functions $U_{f1}, U_{f2}, ..., U_{f35}$ (see Table I). In this section, we show how to construct the 35 f-controlled phase gates, by using single-qubit σ_z gates, two-qubit CP gates, and two-target-qubit CP gates.

$U_{f1}: f(x_1)=f(x_2)=f(x_3)=f(x_4)=0,$	$U_{f19}: f(x_1)=f(x_3)=f(x_4)=f(x_8)=0$
$U_{f2}: f(x_1)=f(x_2)=f(x_3)=f(x_5)=0,$	$U_{f20}: f(x_1)=f(x_3)=f(x_5)=f(x_6)=0$
$U_{f3}: f(x_1)=f(x_2)=f(x_3)=f(x_6)=0,$	$U_{f21}: f(x_1)=f(x_3)=f(x_5)=f(x_7)=0$
$U_{f4}: f(x_1)=f(x_2)=f(x_3)=f(x_7)=0,$	$U_{f22}: f(x_1)=f(x_3)=f(x_5)=f(x_8)=0$
$U_{f5}: f(x_1)=f(x_2)=f(x_3)=f(x_8)=0,$	$U_{f23}: f(x_1)=f(x_3)=f(x_6)=f(x_7)=0$
$U_{f6}: f(x_1)=f(x_2)=f(x_4)=f(x_5)=0,$	$U_{f24}: f(x_1)=f(x_3)=f(x_6)=f(x_8)=0$
$U_{f7}: f(x_1)=f(x_2)=f(x_4)=f(x_6)=0,$	$U_{f25}: f(x_1)=f(x_3)=f(x_7)=f(x_8)=0$
$U_{f8}: f(x_1)=f(x_2)=f(x_4)=f(x_7)=0,$	$U_{f26}: f(x_1)=f(x_4)=f(x_5)=f(x_6)=0$
$U_{f9}: f(x_1)=f(x_2)=f(x_4)=f(x_8)=0,$	$U_{f27}: f(x_1)=f(x_4)=f(x_5)=f(x_7)=0$
$U_{f10}: f(x_1)=f(x_2)=f(x_5)=f(x_6)=0,$	$U_{f28}: f(x_1)=f(x_4)=f(x_5)=f(x_8)=0$
$U_{f11}: f(x_1)=f(x_2)=f(x_5)=f(x_7)=0,$	$U_{f29}: f(x_1)=f(x_4)=f(x_6)=f(x_7)=0$
$U_{f12}: f(x_1)=f(x_2)=f(x_5)=f(x_8)=0,$	$U_{f30}: f(x_1)=f(x_4)=f(x_6)=f(x_8)=0$
$U_{f13}: f(x_1)=f(x_2)=f(x_6)=f(x_7)=0,$	$U_{f31}: f(x_1)=f(x_4)=f(x_7)=f(x_8)=0$
$U_{f14}: f(x_1)=f(x_2)=f(x_6)=f(x_8)=0,$	$U_{f32}: f(x_1)=f(x_5)=f(x_6)=f(x_7)=0$
$U_{f15}: f(x_1)=f(x_2)=f(x_7)=f(x_8)=0,$	$U_{f33}: f(x_1)=f(x_5)=f(x_6)=f(x_8)=0$
$U_{f16}: f(x_1)=f(x_3)=f(x_4)=f(x_5)=0,$	$U_{f34}: f(x_1)=f(x_5)=f(x_7)=f(x_8)=0$
$U_{f17}: f(x_1)=f(x_3)=f(x_4)=f(x_6)=0,$	$U_{f35}: f(x_1)=f(x_6)=f(x_7)=f(x_8)=0$
$U_{f18}: f(x_1)=f(x_3)=f(x_4)=f(x_7)=0,$	

TABLE I: List of the 35 balanced functions for a three-qubit refined Deutsch-Jozsa quantum algorithm. Here, $x_1 = 000, x_2 = 001, x_3 = 010, x_4 = 011, x_5 = 100, x_6 = 101, x_7 = 110$, and $x_8 = 111$. For simplicity, we only list the funtion values, which are "0", for four inputs corresponding to each balanced function. Note that for each balanced function, the function values for the other four inputs (not listed) take a value "1". For instance, for the balanced function corresponding to U_{f1}, the function values for the other four inputs (not listed) are $f(x_5) = f(x_6) = f(x_7) = f(x_8) = 1$.

A single qubit σ_z gate results in the transformation $\sigma_z |0\rangle = |0\rangle$ while $\sigma_z |1\rangle = -|1\rangle$. A two-qubit CP gate C_{jk} on qubits j and k considered here is described as follows

$$|mn\rangle_{jk} \rightarrow (-1)^{m\times n} |mn\rangle_{jk}; \ m, n \in \{0, 1\} \tag{2}$$

which implies that if and only if the control qubit j (the first qubit) is in the state $|1\rangle$, a phase flip happens to the state $|1\rangle$ of the target qubit k (the second qubit), but nothing happens otherwise. In addition, a two-target-qubit CP gate T_{jkl} with the control qubit j and the two target qubits k and l is defined below

$$|mnr\rangle_{jkl} \rightarrow (-1)^{m\times n} (-1)^{m\times r} |mnr\rangle_{jkl}; \ m, n, r \in \{0, 1\} \tag{3}$$

which shows that if and only if the control qubit j (the first qubit) is in the state $|1\rangle$, a

Type 1		
$U_{f1} = \sigma_{z1}$	$U_{f15} = \sigma_{z1}\sigma_{z2}$	$U_{f29} = \sigma_{z1}\sigma_{z2}\sigma_{z3}$
$U_{f10} = \sigma_{z2}$	$U_{f24} = \sigma_{z1}\sigma_{z3}$	
$U_{f21} = \sigma_{z3}$	$U_{f28} = \sigma_{z2}\sigma_{z3}$	
Type 2		
$U_{f5} = C_{23}\sigma_{z1}$	$U_{f13} = C_{13}\sigma_{z1}\sigma_{z2}$	$U_{f27} = C_{12}\sigma_{z2}\sigma_{z3}$
$U_{f12} = C_{13}\sigma_{z2}$	$U_{f17} = C_{23}\sigma_{z1}\sigma_{z3}$	$U_{f30} = C_{12}\sigma_{z1}\sigma_{z2}\sigma_{z3}$
$U_{f22} = C_{12}\sigma_{z3}$	$U_{f23} = C_{12}\sigma_{z1}\sigma_{z3}$	$U_{f31} = C_{13}\sigma_{z1}\sigma_{z2}\sigma_{z3}$
$U_{f8} = C_{23}\sigma_{z1}\sigma_{z2}$	$U_{f26} = C_{13}\sigma_{z2}\sigma_{z3}$	$U_{f35} = C_{23}\sigma_{z1}\sigma_{z2}\sigma_{z3}$
Type 3		
$U_{f3} = T_{312}\sigma_{z1}$	$U_{f16} = T_{213}\sigma_{z3}$	$U_{f19} = T_{312}\ \sigma_{z1}\sigma_{z3}$
$U_{f4} = T_{213}\ \sigma_{z1}$	$U_{f20} = T_{123}\sigma_{z3}$	$U_{f25} = T_{123}\sigma_{z1}\sigma_{z3}$
$U_{f6} = T_{312}\sigma_{z2}$	$U_{f9} = T_{213}\sigma_{z1}\sigma_{z2}$	$U_{f33} = T_{312}\sigma_{z2}\sigma_{z3}$
$U_{f11} = T_{123}\sigma_{z2}$	$U_{f14} = T_{123}\sigma_{z1}\sigma_{z2}$	$U_{f34} = T_{213}\sigma_{z2}\sigma_{z3}$
Type 4		
$U_{f2} = T_{123}C_{23}$	$U_{f18} = T_{123}C_{23}\sigma_{z1}\sigma_{z3}$	$U_{f32} = T_{123}C_{23}\sigma_{z2}\sigma_{z3}$
$U_{f7} = T_{123}C_{23}\sigma_{z1}\sigma_{z2}$		

TABLE II: List of 35 f-controlled phase gates for a three-qubit refined Deutsch-Jozsa quantum algorithm. Here, σ_{z_j} represents a single-qubit σ_{z_j} gate on qubit j ($j = 1, 2, 3$); C_{jk} indicates a two-qubit controlled-phase gate on qutrits j and k ($j, k = 1, 2, 3$), described by Eq. (2); and T_{jkl} is a two-target-qubit CP gate described by Eq. (3).

phase flip happens to the state $|1\rangle$ of the target qubit k (the second qubit) and the state $|1\rangle$ of the target qubit l (the last qubit).

The construction for each of the 35 f-controlled phase gates is listed in Table II. One can see from Table II that the 35 f-controlled phase gates $U_{f1}, U_{f2}, ..., U_{f35}$ are classified into the following four types: (i) Type 1 includes seven f-controlled phase gates each constructed with single-qubit σ_z gates only; (ii) Type 2 contains twelve f-controlled phase gates each constructed with single-qubit σ_z gates and one two-qubit CP gate; (iii) Type 3 has twelve f-controlled phase gates each constructed by using single-qubit σ_z gates and a two-target-qubit CP gate; and (iv) Type 4 involves four f-controlled phase gates each implemented with single-qubit σ_z gates, a two-qubit CP gate, and a two-target-qubit CP gate at most.

IV. IMPLEMENTATION OF THE THREE-QUBIT REFINED DJ ALGORITHM IN CIRCUIT QED

Using the protocol, we now discuss how to implement the three-qubit refined DJ algorithm with three superconducting transmon qutrits $(1, 2, 3)$ each having three levels (i.e., the ground $|0\rangle$, the first excited $|1\rangle$, and the second excited level $|2\rangle$). We then estimate the fidelity of the operation, which is performed in a setup composed of three phase qutrits and a one-dimensional coplanar waveguide resonator.

A. Implementing the algorithm

Since the f-controlled phase gates belonging to Type 1 are constructed using single-qubit gates only, their implementation does not require entanglement and thus can be realized in a classical way. Therefore, in the following we focus on the f-controlled phase gates belonging to Type 2, Type 3, and Type 4. Without loss of generality, let us consider the three f-controlled phase gates U_{f30} (belonging to Type 2), U_{f9} (belonging to Type 3), and U_{f7} (belonging to Type 4). By comparing them with other f-controlled phase gates in the same types, it can be found that these three unitary gates U_{f30}, U_{f9}, and U_{f7} contain the same number of two-qubit CP gates or/and two-target-qubit CP gates but a greater or equal number of single-qubit gates than the other f-controlled phase gates in the same types. Hence, if the three f-controlled phase gates U_{f30}, U_{f9}, and U_{f7} can be implemented, then other f-controlled phase gates in the same types can be achieved with a higher or equal fidelity. In this sense, to see how well the proposal works, it would be sufficient to explore the implementation feasibility of the following three joint quantum operations, described by

$$\begin{aligned} U_1 &= H^{\otimes 3} U_{f30} H^{\otimes 3} = H^{\otimes 3} C_{12} \sigma_{z1} \sigma_{z2} \sigma_{z3} H^{\otimes 3}, \\ U_2 &= H^{\otimes 3} U_{f9} H^{\otimes 3} = H^{\otimes 3} T_{213} \sigma_{z1} \sigma_{z2} H^{\otimes 3}, \\ U_3 &= H^{\otimes 3} U_{f7} H^{\otimes 3} = H^{\otimes 3} T_{123} C_{23} \sigma_{z1} \sigma_{z2} H^{\otimes 3}, \end{aligned} \tag{4}$$

where the gate operation sequence is from right to left. The U_1, U_2, and U_3 here are constructed, according to Fig. 1 and the decomposition of U_{f30}, U_{f9}, and U_{f7} given in Table II. From Eq. (4), one can see that U_1, U_2, and U_3 are implemented through the single-qubit σ_z and H gates, two-qubit CP gates and two-target-qubit CP gates.

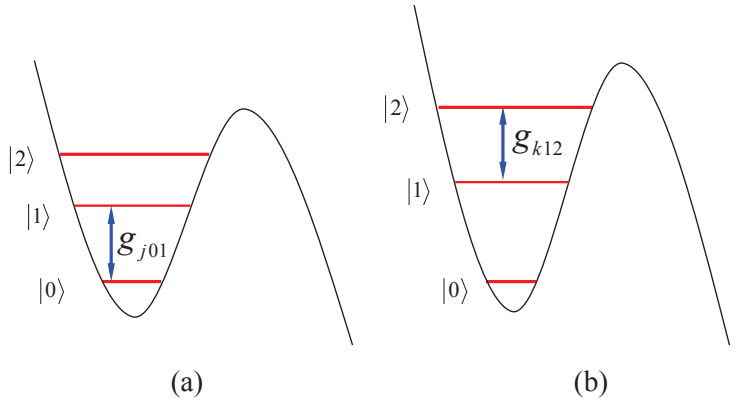

FIG. 2: (Color online) Illustration of qutrit-cavity resonant interaction. (a) The cavity is resonant with the $|0\rangle \leftrightarrow |1\rangle$ transition of qutrit j with a coupling constant g_{j01}. (b) The cavity is resonant with the $|1\rangle \leftrightarrow |2\rangle$ transition of qutrit k with a coupling constant g_{k12}.

A.1 Implementing single-qubit gates—The single-qubit Hamardard H gate or σ_z gate on qutrit j can be realized by applying a pulse resonant with the $|0\rangle \leftrightarrow |1\rangle$ transition of qutrit j ($j = 1, 2, 3$). To eliminate the leakage into the level $|2\rangle$, one can employ the DRAG pulse [34,35], which can reduce the gate error by an order of magnitude relative to the state of the art, all based on smooth and feasible pulse shapes [34]. In addition, to shorten the gate time, the three joint Hamardard gates $H^{\otimes 3}$ in Eq. (4) are performed simultaneously, which can be achieved by turning on and off the pulses applied to the three qutrits at the same time. In the same manner, the three σ_z gates involved in U_1 (the two σ_z gates in U_2 and U_3) are performed simultaneously.

Detailed discussion of how to implement the H gate or σ_z gate is omitted here since implementing a single-qubit gate depends on the use of the pulse shapes and is straightforward in experiments.

A.2 Implementing a two-qubit CP gate— We define g_{j01} (g_{k12}) as the resonant coupling constant between the cavity mode and the $|0\rangle \leftrightarrow |1\rangle$ ($|1\rangle \leftrightarrow |2\rangle$) transition of qutrit j (k). The cavity is initially in the vacuum state $|0\rangle_c$. The procedure for realizing C_{jk} is listed as follows:

Step (i). Adjust the level spacings of qutrit j such that the $|0\rangle \leftrightarrow |1\rangle$ transition is on resonance with the cavity [Fig. 2(a)]. After an interaction time $t_1 = \pi/(2g_{j01})$, the state $|1\rangle_j |0\rangle_c$ changes to $-i|0\rangle_j |1\rangle_c$ while nothing happens to the state $|0\rangle_j |0\rangle_c$ (e.g., see [19]).

Step (ii). Adjust the level spacings of qutrit k such that the $|1\rangle \leftrightarrow |2\rangle$ transition is on

resonance with the cavity [Fig. 2(b)]. After an interaction time $t_2 = \pi/g_{k12}$, the state $|1\rangle_k |1\rangle_c$ becomes $-|1\rangle_k |1\rangle_c$ while the states $|0\rangle_k |0\rangle_c$, $|1\rangle_k |0\rangle_c$ and $|0\rangle_k |1\rangle_c$ remain unchanged.

Step (iii). Adjust the level spacings of qutrit j such that the $|0\rangle \leftrightarrow |1\rangle$ transition is on resonance with the cavity [Fig. 2(a)]. After an interaction time $t_3 = 3\pi/(2g_{j01})$, the state $|0\rangle_j |1\rangle_c$ changes to $i|1\rangle_j |0\rangle_c$ while nothing happens to the state $|0\rangle_j |0\rangle_c$.

One can check that the state $|1\rangle_j |0\rangle_k |0\rangle_c$ remains unchanged while the state $|1\rangle_j |1\rangle_k |0\rangle_c$ changes to $-|1\rangle_j |1\rangle_k |0\rangle_c$ after the above operations. On the other hand, the initial states $\{|0\rangle_j |0\rangle_k |0\rangle_c, |0\rangle_j |1\rangle_k |0\rangle_c\}$ remain unchanged during the entire operation above. These results show that a two-qubit CP gate C_{jk}, described by Eq. (2), was achieved with qutrit j (the control) and qutrit k (the target) after the above process, while the cavity returns to its original vacuum state.

A.3 Realizing a two-target-qubit CP gate— By carefully examining the procedure described above for implementing C_{jk}, we note that a two-targe-qubit CP gate T_{jkl} described by Eq. (3) can be realized using four operational steps only:

Steps (i) and (ii): the operations for these two steps are the same as those for steps (i) and (ii) described above.

Step (iii): Adjust the level spacings of qutrit l such that the $|1\rangle \leftrightarrow |2\rangle$ transition is on resonance with the cavity. After an interaction time $t_3 = \pi/g_{l12}$ (where g_{l12} is the coupling constant between the cavity mode and the $|1\rangle \leftrightarrow |2\rangle$ transition of qutrit l), the state $|1\rangle_l |1\rangle_c$ becomes $-|1\rangle_l |1\rangle_c$ while the states $|0\rangle_l |0\rangle_c$, $|1\rangle_l |0\rangle_c$ and $|0\rangle_l |1\rangle_c$ remain unchanged.

Step (iv): the operation for this step is the same as that for step (iii).

During performing single-qubit-gate operations, all three superconducting phase qutrits 1, 2, and 3 need to be decoupled from the cavity mode; and during performing a two-qubit CP gate or a two-target-qubit CP gate, irrelevant qutrits need to be decoupled from the cavity mode. This requirement can be met by a prior adjustment of the level spacings of the qutrits. Note that for superconducting qutrits, the level spacings can be rapidly adjusted by varying external control parameters (e.g., magnetic flux applied to phase, transmon, or flux qutrits; see, e.g., [3,36,37]).

As a final note, it should be mentioned that the method described above for implementing *a two-qubit CP gate* via resonant interaction is not new, which was previously proposed [38,39]. We would like to stress that our focus is to take the resonant interaction as an example to explore the possibility of implementing the three-qubit DJ algorithm with su-

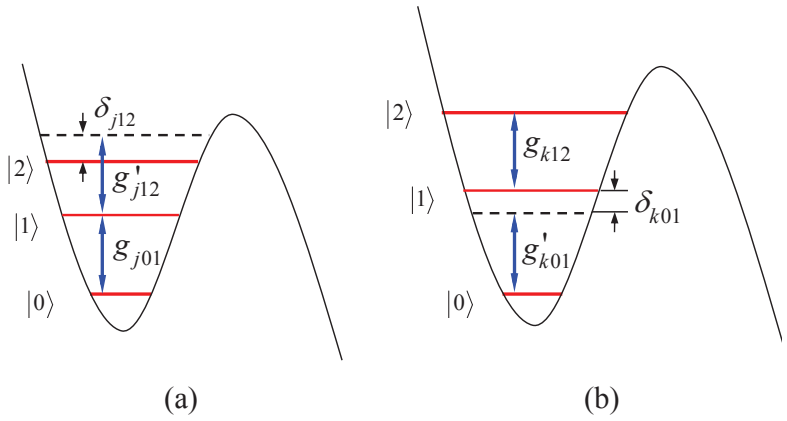

FIG. 3: (Color online) Illustration of qutrit-cavity interaction during the cavity mode interacting with qutrit j or qutrit k ($j, k = 1, 2$, or 3). For the details, see subsection 4.2.

perconducting transmon qutrits coupled to a single cavity, by using the protocol presented in the previous section.

B. Fidelity

Let us now study the fidelity of the operation. Since the resonant interaction is used in the implementation of the single-qubit H gates or σ_z gates, these basic gates can be completed within a very short time (e.g., by increasing the pulse Rabi frequency). In addition, as mentioned previously, one can apply the DRAG pulses to eliminate the leakage into the level $|2\rangle$. Thus, the single-qubit gate error is negligibly small. In this case, decoherence of the system would have a negative impact on the operation of implementing a two-qubit CP gate as well as a two-target-qubit CP gate, due to the population of the cavity photons during the operation. As discussed above, the implementation of these CP gates involves two basic operations:

(i) The first one requires that during performing C_{jk} and T_{jkl}, the cavity mode is resonant with the $|0\rangle \rightarrow |1\rangle$ transition of the control qutrit j. In realistic case, the interaction Hamiltonian for this basic operation is given by

$$H_{I,1} = \left(g_{j01}a^{+}S_{j01}^{-} + h.c.\right) + \left(g'_{j12}e^{-i\delta_{j12}t}a^{+}S_{j12}^{-} + h.c.\right), \tag{5}$$

where a^{+} is the photon creation operator of the cavity mode, and the second term represents the unwanted off-resonant coupling between the cavity mode and the $|1\rangle \leftrightarrow |2\rangle$ transition,

with a coupling constant g'_{j12} and a detuning $\delta_{j12} = \omega_{j12} - \omega_c < 0$ [Fig. 3(a)].

(ii) The second one requires that during performing C_{jk} and T_{jkl}, the cavity mode is resonant with the $|1\rangle \leftrightarrow |2\rangle$ transition of the target qutrit k. The interaction Hamiltonian for this basic operation is given by

$$H_{I,2} = \left(g_{k12} a^+ S^-_{k12} + h.c.\right) + \left(g'_{k01} e^{-i\delta_{k01} t} a^+ S^-_{k01} + h.c.\right), \tag{6}$$

where the second term represents the unwanted off-resonant coupling between the cavity mode and the $|0\rangle \leftrightarrow |1\rangle$ transition, with a coupling constant g'_{k01} and a detuning $\delta_{k01} = \omega_{k01} - \omega_c > 0$ [Fig. 3(b)].

As discussed previously, the cavity mode needs to be resonant with the $|1\rangle \rightarrow |2\rangle$ transition of the target qutrit l during performing T_{jkl}. Note that the Hamiltonian governing this basic operation is the same as $H_{I,2}$ with a replacement of the index k by l.

It should be mentioned that the term describing the pulse-induced or the cavity-induced coherent $|0\rangle \leftrightarrow |2\rangle$ transition for each qutrit is not included in the Hamiltonians $H_{I,1}$ and $H_{I,2}$, since this transition is negligible because of $\omega, \omega_c \ll \omega_{j02}, \omega_{k02}$ $(j, k = 1, 2, 3)$ (Fig. 3).

For each of the two basic types of operations described above, the dynamics of the lossy system, composed of three qutrits $(1, 2, 3)$ and the cavity, is determined by

$$\begin{aligned}
\frac{d\rho}{dt} \;=\; & -i\left[H_I, \rho\right] + \kappa \mathcal{L}\left[a\right] \\
& + \sum_{j=1}^{3} \left\{ \gamma_{j21} \mathcal{L}\left[S^-_{j21}\right] + \gamma_{j20} \mathcal{L}\left[S^-_{j20}\right] + \gamma_{j10} \mathcal{L}\left[S^-_{j10}\right] \right\} \\
& + \sum_{j=1}^{3} \gamma_{j,\varphi 2} \left(S_{j22} \rho S_{j22} - S_{j22}\rho/2 - \rho S_{j22}/2 \right) \\
& + \sum_{j=1}^{3} \gamma_{j,\varphi 1} \left(S_{j11} \rho S_{j11} - S_{j11}\rho/2 - \rho S_{j11}/2 \right),
\end{aligned} \tag{7}$$

where H_I is the $H_{I,1}$ or $H_{I,2}$ above, j represents qutrit j $(j = 1, 2, 3)$, $S^-_{j20} = |0\rangle_j \langle 2|$, $S_{j22} = |2\rangle_j \langle 2|$, $S_{j11} = |1\rangle_j \langle 1|$, $\mathcal{L}\left[a\right] = \Lambda\rho\Lambda^+ - \Lambda^+\Lambda\rho/2 - \rho\Lambda^+\Lambda/2$ with $\Lambda = a, S^-_{j21}, S^-_{j20}, S^-_{j10}$. In addition, κ is the decay rate of the cavity mode, $\gamma_{j21,}$ γ_{j20}, and γ_{10} are, respectively, the energy relaxation rates of the level $|2\rangle$ of qutrit j for the decay paths $|2\rangle \rightarrow |1\rangle$, $|2\rangle \rightarrow |0\rangle$, and $|1\rangle \rightarrow |0\rangle$, and $\gamma_{j,\varphi 2}$ $(\gamma_{j,\varphi 1})$ is the dephasing rate of the level $|2\rangle$ $(|1\rangle)$ of qutrit j.

The fidelity of the operation is given by [40]

$$\mathcal{F} = \sqrt{\langle \psi_{id} | \, \widetilde{\rho} \, | \psi_{id} \rangle}, \tag{8}$$

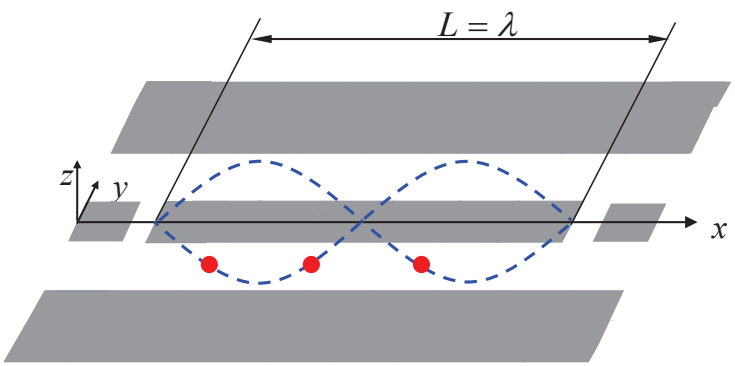

FIG. 4: (color online) Setup for three superconducting transmon qutrits (red dots), and a (grey) standing-wave one-dimensional coplanar waveguide resonator. L is the length of the resonator, and λ is the wavelength of the resonator mode. The two (blue) curved lines represent the standing wave magnetic field in the z-direction.

where $|\psi_{id}\rangle$ is the output state of an ideal system (i.e., without dissipation and dephasing) after a joint operation U_1, U_2, or U_3 is performed on the qutrit system initially in the state $|000\rangle$ and the cavity mode initially in the vacuum state $|0\rangle_c$, which is given by

$$\begin{aligned} U_1 \ &: \ |\psi_{id}\rangle = \frac{1}{2}\left(-|001\rangle + |011\rangle + |101\rangle + |111\rangle\right) \otimes |0\rangle_c \\ U_2 \ &: \ |\psi_{id}\rangle = \frac{1}{2}\left(-|001\rangle + |011\rangle + |100\rangle + |110\rangle\right) \otimes |0\rangle_c \\ U_3 \ &: \ |\psi_{id}\rangle = \frac{1}{2}\left(-|001\rangle + |010\rangle + |100\rangle + |111\rangle\right) \otimes |0\rangle_c , \end{aligned} \tag{9}$$

while $\widetilde{\rho}$ is the final density operator of the whole system when the gate operations are performed in a realistic physical system.

We now numerically calculate the fidelity of the joint operations U_1, U_2, and U_3, for a setup shown in Fig. 4. Without loss of generality, let us consider three identical transmon qutrits. In this case, we can drop off the first subscript (j,k,l) for the detunings, Rabi frequencies, and coupling constants. For simplicity, we assume that $g_{01} \sim g'_{01} = g$. One has $g_{12} \sim g'_{12} \sim \sqrt{2}g$ for the transmon qutrit here [41]. Choose $g/(2\pi) \sim 15$ MHz, which can be reached for a superconducting transmon qutrit coupled to a one-dimensional standing-wave CPW (coplanar waveguide) resonator [42]. Other parameters used in the numerical calculation are as follows: $\gamma_{j,\varphi 2}^{-1} = \gamma_{j,\varphi 1}^{-1} = 10$ μs, $\gamma_{21}^{-1} = 15$ μs, $\gamma_{20}^{-1} = 150$ μs [43], $\gamma_{10}^{-1} = 20$ μs, and $\kappa^{-1} = 5$ μs. Define $b_0 = \delta_{01}/g'_{01}$ and $b_1 = -\delta_{12}/g'_{12}$. For simplicity, we choose $b_1 = 10$. For the parameters chosen above, the fidelity versus b_0 is shown in Fig. 5, from which one

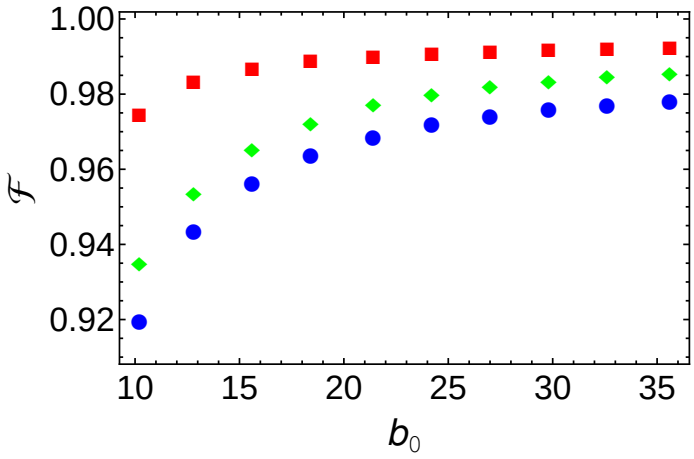

FIG. 5: (Color online) Fidelity versus b_0. Here, $b_0 = \delta_{01}/g'_{01}$, and the red squares, green diamonds, and blue circles correspond to the joint operations U_1, U_2, and U_3 given in Eq. (4), respectively. Refer to the text for the parameters used in the numerical calculation.

can see that for $b_0 = 24$, a high fidelity $\sim 99.1\%$, 98.0%, and 97.2% can be achieved for the joint operations U_1, U_2, and U_3, respectively. We remark that the fidelity can be further increased by improving system parameters.

For $b_0 = 24$ and $b_1 = 10$, we have $-\delta_{12} \sim 0.21$ GHz, $\delta_{01} \sim 0.36$ GHz, which is achieved in experiments [44]. T_1 and T_2 can be made to be on the order of $20 - 60$ μs for state-of-the-art superconducting transom devices [4]. For superconducting transmon qutrits, the typical transition frequency between two neighbor levels is between 4 and 10 GHz [6,21,23,24]. As an example, let us consider a cavity with frequency $\nu_c \sim 6$ GHz. Thus, for the κ^{-1} used in the numerical calculation, the required quality factor for the cavity is $Q \sim 1.9 \times 10^5$. Note that superconducting CPW resonators with a loaded quality factor $Q \sim 10^6$ have been experimentally demonstrated [45,46], and planar superconducting resonators with internal quality factors above one million ($Q > 10^6$) have also been reported recently [47]. Our analysis given here demonstrates that implementation of the three-qubit refined DJ algorithm is feasible within the present circuit QED technique.

V. CONCLUSION

We have proposed a protocol for constructing the 35 f-controlled phase gates of a three-qubit refined DJ algorithm, by using single-qubit σ_z gates, two-qubit CP gates and two-target-qubit CP gates. Using this protocol, we have discussed how to implement the three-qubit refined DJ algorithm with superconducting transmon qutrits resonantly coupled to a cavity. Our numerical calculation shows that implementation of this quantum algorithm is feasible for the current circuit QED. Finally, it is noted that this protocol is quite general and can be applied to implement the three-qubit refined Deutsch-Jozsa algorithm in various of physical systems.

ACKNOWLEDGMENTS

C.P.Y. was supported in part by the National Natural Science Foundation of China under Grant Nos. 11074062 and 11374083, the Zhejiang Natural Science Foundation under Grant No. LZ13A040002, and the funds from Hangzhou Normal University under Grant Nos. HSQK0081 and PD13002004. Q.P.S. was supported by the Zhejiang Provincial Natural Science Foundation of China under Grant No. LQ12A05004. This work was also supported by the funds from Hangzhou City for the Hangzhou-City Quantum Information and Quantum Optics Innovation Research Team.

---

[1] A. Blais, R. S. Huang, A. Wallraff, S. M. Girvin, and R. J. Schoelkopf, Cavity quantum electrodynamics for superconducting electrical circuits: An architecture for quantum computation, Phys. Rev. A **69**, 062320 (2004).

[2] J. Q. You and F. Nori, Atomic physics and quantum optics using superconducting circuits,Nature (London) **474**, 589 (2011); P. D. Nation, J. R. Johansson, M. P. Blencowe, and F. Nori, Colloquium: Stimulating uncertainty: Amplifying the quantum vacuum with superconducting circuits, Rev. Mod. Phys. **84**, 1 (2012); Z. L. Xiang, S. Ashhab, J. Q. You, and F. Nori, Hybrid quantum circuits: Superconducting circuits interacting with other quantum systems, Rev. Mod. Phys. **85**, 623 (2013).

[3] J. Clarke and F. K. Wilhelm, Superconducting quantum bits, Nature (London) **453**, 1031 (2008).

[4] J. B. Chang *et al.*, Improved superconducting qubit coherence using titanium nitride, Appl. Phys. Lett. **103**, 012602 (2013); H. Paik *et al.*, Observation of High Coherence in Josephson Junction Qubits Measured in a Three-Dimensional Circuit QED Architecture, Phys. Rev. Lett. **107**, 240501 (2011); J. M. Chow *et al.*, Implementing a strand of a scalable fault-tolerant quantum computing fabric, Nature Communications **5**, 4015 (2014).

[5] C. P. Yang, S. I. Chu and S. Han, Possible realization of entanglement, logical gates, and quantum-information transfer with superconducting-quantum-interference-device qubits in cavity QED, Phys. Rev. A **67**, 042311 (2003).

[6] J. Majer *et al.*, Coupling superconducting qubits via a cavity bus, Nature (London) **449**, 443 (2007).

[7] L. DiCarlo *et al.*, Demonstration of two-qubit algorithms with a superconducting quantum processor, Nature (London) **460**, 240 (2009).

[8] C. P. Yang, S. I. Chu and S. Han, Quantum Information Transfer and Entanglement with SQUID Qubits in Cavity QED: A Dark-State Scheme with Tolerance for Nonuniform Device Parameter, Phys. Rev. Lett. **92**, 117902 (2004).

[9] I. Chiorescu et al., Coherent dynamics of a flux qubit coupled to a harmonic oscillator, Nature (London) **431**, 159 (2004).

[10] A. Wallraff et al., Strong coupling of a single photon to a superconducting qubit using circuit quantum electrodynamics, Nature (London) **431**, 162 (2004).

[11] J. Q. You and F. Nori, Quantum information processing with superconducting qubits in a microwave field, Phys. Rev. B **68**, 064509 (2003).

[12] C. P. Yang, S. I. Chu and S. Han, Simplified realization of two-qubit quantum phase gate with four-level systems in cavity QED, Phys. Rev. A **70**, 044303 (2004); J. of Phys.: Cond. Mat. **16**, 1907 (2004); X. L. He *et al.,* Quantum logical gates with four-level superconducting quantum interference devices coupled to a superconducting resonator, Phys. Rev. A **82**, 024301 (2010).

[13] P. Zhang, Z. D. Wang, J. D. Sun, and C. P. Sun, Holonomic quantum computation using rf superconducting quantum interference devices coupled through a microwave cavity, Phys. Rev. A **71**, 042301 (2005).

[14] S. L. Zhu, Z. D. Wang, and P. Zanardi, Geometric Quantum Computation and Multiqubit

Entanglement with Superconducting Qubits inside a Cavity, Phys. Rev. Lett. **94**, 100502 (2005).

[15] K. H. Song, Z. W. Zhou, and G. C. Guo, Quantum logic gate operation and entanglement with superconducting quantum interference devices in a cavity via a Raman transition, Phys. Rev. A **71**, 052310 (2005).

[16] Z. B. Feng, Coupling charge qubits via Raman transitions in circuit QED, Phys. Rev. A **78**, 032325 (2008).

[17] S. Saito, T. Tilma, S. J. Devitt, K. Nemoto, and K. Semba, Experimentally realizable controlled NOT gate in a flux qubit/resonator system, Phys. Rev. B **80**, 224509 (2009).

[18] G. Haak, F. Helmer, M. Mariantona, F. Marquardt, and E. Solano, Resonant quantum gates in circuit quantum electrodynamics, Phys. Rev. B. **82**, 024514 (2010).

[19] C. P. Yang and S. Han, n-qubit-controlled phase gate with superconducting quantum-interference devices coupled to a resonator, Phys. Rev. A **72**, 032311 (2005); **73**, 032317 (2006).

[20] C. P. Yang, Y. X. Liu, and F. Nori, Phase gate of one qubit simultaneously controlling n qubits in a cavity, Phys. Rev. A **81**, 062323 (2010); C. P. Yang, S. B. Zheng, and F. Nori, Multiqubit tunable phase gate of one qubit simultaneously controlling n qubits in a cavity, Phys. Rev. A **82**, 062326 (2010).

[21] P. J. Leek, S. Filipp, P. Maurer, M. Baur, R. Bianchetti, J. M. Fink, M. Goppl, L. Steffen, and A. Wallraff, Using sideband transitions for two-qubit operations in superconducting circuits, Phys. Rev. B **79**, 180511(R) (2009).

[22] E. Lucero *et al.*, Computing prime factors with a Josephson phase qubit quantum processor, arXiv:1202.5707.

[23] A. Fedorov, L. Steffen, M. Baur, M. P. daSilva, and A. Wallraff, Implementation of a Toffoli gate with superconducting circuits, Nature (London) **481**, 170 (2012).

[24] M. D. Reed *et al.*, Realization of three-qubit quantum error correction with superconducting circuits, Nature (London) **482**, 382 (2012).

[25] M. Mariantoni *et al.*, Implementing the Quantum von Neumann Architecture with Superconducting Circuits, Science **334**, 61 (2011).

[26] P. W. Shor, Algorithms for quantum computation: discrete logarithms and factoring, in Proceedings of the 35th Annual Symposium on Foundation of Computer Science (IEEE Computer

Society, Los Alamos, CA, 1994), p. 124.

[27] L. K. Grover, Quantum Mechanics Helps in Searching for a Needle in a Haystack, Phys. Rev. Lett. **79**, 325 (1997).

[28] D. Deutsch, Quantum Theory, the Church-Turing Principle and the Universal Quantum Computer, Proc. R. Soc. London Scr. A **400**, 97 (1985); D. Deutsch, Quantum Computational Networks, Proc. R. Soc. London Scr. A **425**, 73 (1989).

[29] D. Deutsch and R. Jozsa, Rapid Solution of Problems by Quantum Computation, Proc. R. Soc. London Scr. A **439**, 553 (1992).

[30] P. Shor, Polynomial-Time Algorithms for Prime Factorization and Discrete Logarithms on a Quantum Computer, SIAM J. Comput. **26**, 1484 (1997).

[31] D. Simon, On the power of quantum computation, Proc. 35th Annual Symposium on Foundations of Computer Science, IEEE Computer Society Press, Los Alamitos, CA, 116 (1994).

[32] L. Grover, A Fast Quantum Mechanical Algorithm for Database Search, Proc. 28th Annual ACM Symposium on Theory of Computing, ACM Press, New York, 212 (1996).

[33] D. Collins, K. W. Kim, and W. C. Holton, Deutsch-Jozsa algorithm as a test of quantum computation, Phys. Rev. A **58**, 1633(R) (1998).

[34] F. Motzoi, J. M. Gambetta, P. Rebentrost, and F. K. Wilhelm, Simple Pulses for Elimination of Leakage in Weakly Nonlinear Qubits, Phys. Rev. Lett. **103**, 110501 (2009).

[35] Erik Lucero *et al.*, Reduced phase error through optimized control of a superconducting qubit, Phys. Rev. A **82**, 042339 (2010).

[36] S. Han, J. Lapointe, and J. E. Lukens, in Single-Electron Tunneling and Mesoscopic Devices, Springer Series in Electronics and Photonics, Vol. **31** (Springer, Berlin, 1991), pp. 219 – 222.

[37] M. Neeley, M. Ansmann, R. C. Bialczak, M. Hofheinz, N. Katz, E. Lucero, A. OConnell, H. Wang, A. N. Cleland, and J. M. Martinis, Process tomography of quantum memory in a Josephson-phase qubit coupled to a two-level state, Nature Phys. **4**, 523 (2008).

[38] A. Rauschenbeutel, G. Nogues, S. Osnaghi, P. Bertet, M. Brune, J. M. Raimond, and S. Haroche, Coherent operation of a tunable quantum phase gate in cavity QED, Phys. Rev. Lett. 83, 5166 (1999).

[39] M. S. Sherwin, A. Imamoglu, and T. Montroy, Quantum computation with quantum dots and terahertz cavity quantum electrodynamics, Phys. Rev. A 60, 3508 (1999).

[40] M. A. Nielsen and I. L. Chuang, Quantum Computation and Quantum Information (Cam-

bridge University Press, Cambridge, England, 2001).

[41] J. Koch, T. M. Yu, J. Gambetta, A. A. Houck, D. I. Schuster, J. Majer, A. Blais, M. H. Devoret, S. M. Girvin, and R. J. Schoelkopf, Charge-insensitive qubit design derived from the Cooper pair box, Phys. Rev. A **76**, 042319 (2007).

[42] L. DiCarlo, M. D. Reed, L. Sun, B. R. Johnson, J. M. Chow, J. M. Gambetta, L. Frunzio, S. M. Girvin, M. H. Devoret, and R. J. Schoelkopf, Preparation and measurement of three-qubit entanglement in a superconducting circuit, Nature (London) **467**, 574 (2010).

[43] For a transmon qutrit with the three levels considered, the $|0\rangle \leftrightarrow |2\rangle$ dipole matrix element is much smaller than that of the $|0\rangle \leftrightarrow |1\rangle$ and $|1\rangle \leftrightarrow |2\rangle$ transitions (see [38]). Thus, $\gamma_{20}^{-1} \gg \gamma_{10}^{-1}, \gamma_{21}^{-1}$.

[44] J. A. Schreier *et al.*, Suppressing charge noise decoherence in superconducting charge qubits, Phys. Rev. B **77**, 180502(R) (2008).

[45] W. Chen, D. A. Bennett, V. Patel, and J. E. Lukens, Substrate and process dependent losses in superconducting thin film resonators, Supercond. Sci. Technol. **21**, 075013 (2008).

[46] P. J. Leek, M. Baur, J. M. Fink, R. Bianchetti, L. Steffen, S. Filipp, and A. Wallraff, Cavity Quantum Electrodynamics with Separate Photon Storage and Qubit Readout Modes, Phys. Rev. Lett. **104**, 100504 (2010).

[47] A. Megrant *et al.*, Planar superconducting resonators with internal quality factors above one million, Appl. Phys. Lett. **100**, 113510 (2012).